

## Orbital Spectrum Analysis of Fast Ion drift motion and transport in toroidal magnetic field configurations

G. Anastassiou<sup>1</sup>, P. Zestanakis<sup>1</sup>, Y. Kominis<sup>2</sup>, AUG Team<sup>a</sup>, MST1 Team<sup>b</sup>

<sup>1</sup>*School of Electrical and Computer Engineering, NTUA, Athens, Greece*

<sup>2</sup>*School of Applied Mathematical and Physical Sciences, NTUA, Athens, Greece*

<sup>a</sup>*See author list of H. Meyer et al., 2019 Nucl. Fusion 59 112014*

<sup>b</sup>*See author list of B. Labit et al., 2019 Nucl. Fusion 59 086020*

### Introduction

The dynamics of Energetic Particles (EP) in a fusion reactor is subject to extensive investigation mostly due to their impact on the confinement and heating of the plasma bulk. EPs, by interacting with MHD modes or externally applied magnetic perturbations, undergo an enhanced radial transport which may compromise the heating efficiency of the device. Intense and localized fast ion (FI) bursts can also severely damage the Plasma Facing Components (PFC) and/or the diagnostics.

Although canonical coordinates are widely used in Guiding Center (GC) theory to calculate FI trajectories [1], the prominent advantages of an Action Angle (AA) transformation, is not sufficiently exploited in real tokamak configurations, with explicit calculations carried out only for the simplified cases of Zero-Drift Width (ZDW) approximation of a Large Aspect Ratio (LAR) equilibrium. Our model focuses on the implementation of a Full Drift Width (FuDW) scheme using canonical Hamiltonian theory, where the Actions are calculated by a simple integration of the respective canonical momentum over the phase-space, leading to the characteristic frequencies of the particles. Applying this procedure for all sets of parameters (namely the magnetic moment  $\mu$ , toroidal momentum  $P_\zeta$ , energy  $E$ ) it is possible to construct a multi-dimensional map of the induced frequencies, creating a parametric spectral distribution across the phase space, a process that is readily associated with the underlying resonance conditions of FI interactions.

### Theoretical background

In an axisymmetric toroidal configuration, the Hamiltonian of the interaction is given from the expression  $\mathcal{H} = \rho_{\parallel}^2 B^2 / 2 + \mu B$ , where  $\rho_{\parallel}$  is the velocity component parallel to the axisymmetric magnetic field  $B$ , and  $\mu$  is the magnetic moment. The three sets of canonical coordinates  $(\mu, \zeta)$ ,  $(P_\zeta, \zeta)$ ,  $(P_\theta, \theta)$  are related with  $\psi, \rho_{\parallel}$  resulting in the Hamiltonian [1]

$$\mathcal{H}(\mu, P_\zeta, P_\theta; \zeta, \zeta, \theta) = \frac{[P_\zeta + \psi_p(P_\zeta, P_\theta)]^2}{2g^2(\psi(P_\zeta, P_\theta))} B^2(\psi(P_\zeta, P_\theta), \theta) + \mu B(\psi(P_\zeta, P_\theta), \theta) \quad (1)$$

where  $\psi, \psi_p$  are respectively the toroidal and poloidal fluxes,  $\zeta, \theta$  are the toroidal and poloidal angle-coordinates,  $I, g$ , correspond to the toroidal and poloidal currents and  $P_\theta$  is the canonical poloidal momentum. In our modelling approach, we study the special case of a LAR configuration at low  $\beta$  which forms an approximate cylindrical equilibrium. Keeping only up to first order terms in aspect ratio, we obtain [1]  $I = \delta = 0, g = 1$ , while the magnetic field becomes  $B = B_0(1 - \varepsilon \cos \theta)$ , with  $\varepsilon$  being the ordering parameter of the aspect ratio approximation. Accordingly, the Hamiltonian takes the form

$$\mathcal{H}(\mu, P_\zeta, P_\theta; \zeta, \zeta, \theta) = \frac{1}{2} [P_\zeta + \psi_p(P_\theta)]^2 (1 - \sqrt{2P_\theta} \cos \theta)^2 + \mu (1 - \sqrt{2P_\theta} \cos \theta) \quad (2)$$

For the case of a smooth  $q$  profile we can locally neglect higher order derivatives of  $\psi_p$  with respect to  $\psi = P_\theta$  resulting in a significantly simplified dynamical system.

### Action-Angle formalism under LAR approximation

Introducing a generating function of the general form

$$F(\zeta, \zeta, \theta; J_\zeta, J_\zeta, J_\theta) = -J_\zeta \zeta - J_\zeta \zeta - \int^\theta P_\theta(\theta'; J_\zeta, J_\zeta) d\theta' \quad (3)$$

we obtain the canonical transformation to AA variable pairs  $(\mu, \zeta) \rightarrow (J_\zeta, \hat{\zeta})$ ,  $(P_\zeta, \zeta) \rightarrow (J_\zeta, \hat{\zeta})$   $(P_\theta, \theta) \rightarrow (J_\theta, \hat{\theta})$ . Apparently, two (out of three) Actions coincide with the magnetic moment and the toroidal momentum, whereas the third Action represents the bounce/transit Action of the poloidal motion and is calculated from the expression

$$J_\theta = \frac{1}{2\pi} \oint P_\theta(E, \mu, P_\zeta; \theta) d\theta = \frac{1}{2\pi} \oint P_\theta(E, J_\zeta, J_\zeta; \theta) d\theta \quad (4)$$

while the conjugate Angles, related to the orbital frequencies, are given from [2]

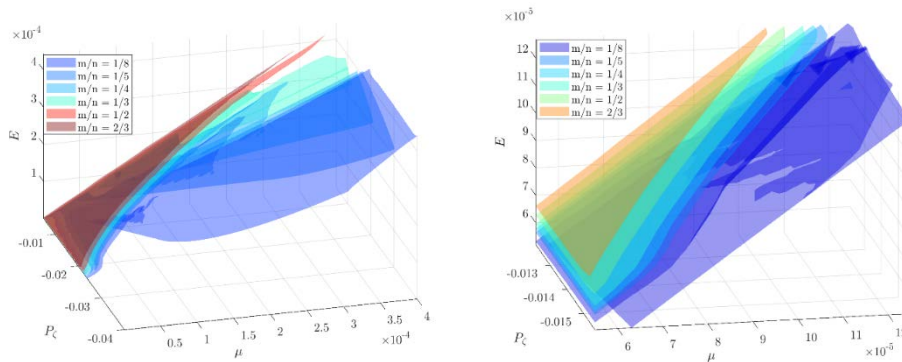


Figure 1 Resonance mapping as function of the constants of motion  $(\mu, P_\zeta, E)$  for the unperturbed orbits corresponding to AUG shot #33127 @ $t=4.35s$  [4] for variables extending through the entire phase-space of the interaction.

$$\dot{\zeta} \equiv \hat{\omega}_\zeta = \frac{\partial \mathcal{H}(\mathbf{J})}{\partial J_\zeta} = -\frac{\partial \mathcal{H}(\mathbf{J})}{\partial J_\theta} \frac{\partial J_\theta}{\partial J_\zeta} \quad \dot{\zeta} \equiv \hat{\omega}_\zeta = \frac{\partial \mathcal{H}(\mathbf{J})}{\partial J_\zeta} = -\frac{\partial \mathcal{H}(\mathbf{J})}{\partial J_\theta} \frac{\partial J_\theta}{\partial J_\zeta} \quad \dot{\theta} \equiv \hat{\omega}_\theta = \frac{\partial \hat{\mathcal{H}}(\mathbf{J})}{\partial J_\theta} \quad (5)$$

with  $\hat{\omega}_\theta$  being the bounce/transit poloidal frequency, and  $\hat{\omega}_\zeta, \hat{\omega}_\zeta$  being the bounce averaged cyclotron and toroidal-drift frequency, respectively. From (5) it is easy to show that

$$\frac{\hat{\omega}_\zeta}{\hat{\omega}_\theta} = \frac{1}{2\pi} (\Delta \zeta)_{T_\theta}, \quad \frac{\hat{\omega}_\zeta}{\hat{\omega}_\theta} = \frac{1}{2\pi} (\Delta \zeta)_{T_\theta} \quad (6)$$

where  $(\Delta \zeta)_{T_\theta}, (\Delta \zeta)_{T_\theta}$  is the variation of  $\zeta, \zeta$ , respectively, within a poloidal period  $T_\theta$ .

Our modelling approach provides a compact semi-analytical formula for bounce/transit averaged dynamics in an axisymmetric toroidal configuration which allows us to express the orbital spectrum of the GC motion as a function of the constant Actions and the Energy, creating a multi-dimensional mapping of the induced resonances of the unperturbed motion. Consequently, it is possible to accurately pinpoint the resonances for a specific set of  $(\mu, P_\zeta, E)$  without the time consuming scan of the entire phase. In Fig.1 we demonstrate such a map for variables extending almost through the entire phase space of the interaction.

The most suitable tool for the validation of our model is the Fast Ion Loss Detector (FILD) installed in AUG [3]. In order to carry out the validation process, we compare the kinetic parameters and the type of the expunging ions of our model with these obtained from FILD experiments. Figure 2 demonstrates the quite accurate predictions of our model regarding the type of the escaping orbits as well as their kinetic parameters [4], while a similar behavior is also witnessed in other FILD-involved shots, as well [3], [6].

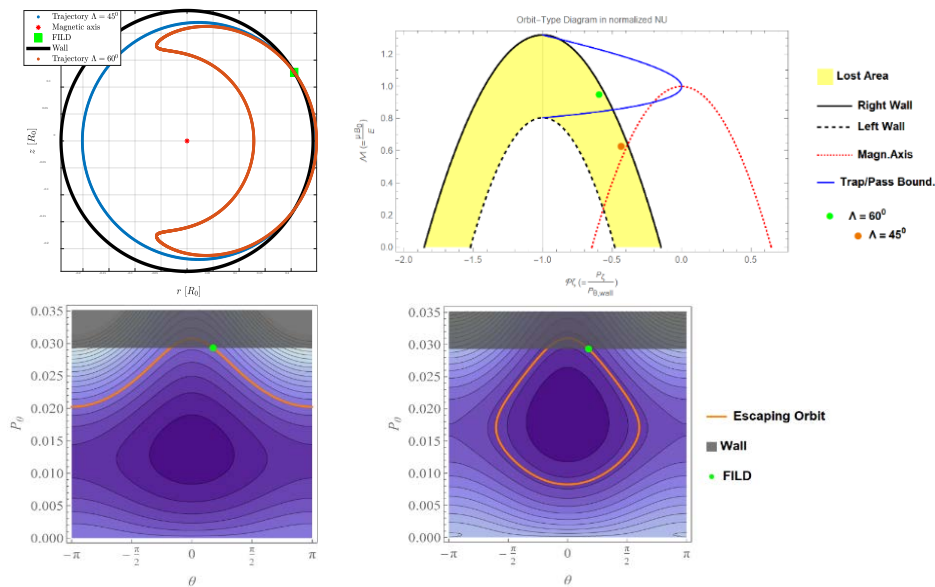


Figure 2 Traces of expunged ions picked up by FILD and reconstructed lost orbits corresponding to the high density FILD spots, for AUG shot #33127 @t=4.35s [4]. The type of the escaping orbits as well as their kinetic parameters are in very good agreement with the reconstructed orbits demonstrated in Fig.5 of Ref.[4]. The barely unconfined orbits for the different values of pitch angle are also shown in both normalized  $\mathcal{M}-P_\zeta$  and  $P_\theta-\theta$  phase space

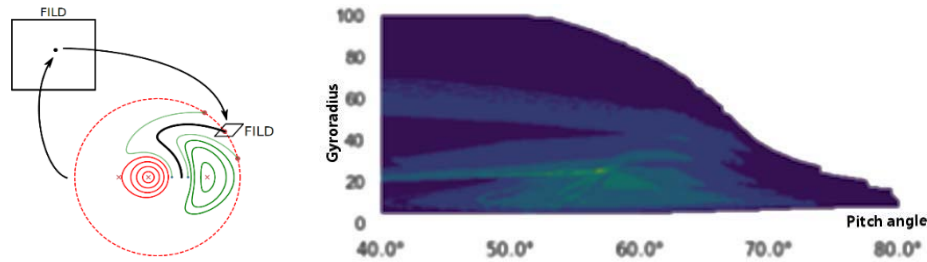


Figure 3. Left: Escaping orbits picked up by FILD. Right:  $P_i$  profiles exhibit an adequate match with FILD profiles of AUG shot #30810 (Fig.9 of Ref.[6])

### Resonance density distribution

The chaotic motion of FI appears in domains around unperturbed orbits which are in resonance with perturbative modes [5] and their extent depends on the strength of the perturbations and can be estimated by means of canonical perturbation theory. Hence, initially confined FIs may end up in FILD's probe when they fall into the chaotic domain of a resonance, however, FI losses will not be affected if no resonant orbit is sufficiently close to the wall. FILD traces are associated with a single escaping orbit, which belongs to a family of orbits with the same  $(\mu, P_\zeta)$ . The projection of any such family on the poloidal plane is called *poloidal slice* (Fig. 3). Accordingly, the probability of an escaping ion to be picked up by FILD in the presence of a perturbation is characterized by the number of resonant orbits in the slice  $n_{res}$ , and the maximum toroidal flux surface crossed by the resonant orbits  $\psi_{max}$ , and can be estimated through the *resonance index*

$$P_i = n_{res} \psi_{max} \quad (7)$$

$P_i$  profile provides an estimation of FI populations whose confinement may be lost (Fig.3). It relies solely on unperturbed resonant orbits quantities, and as such, may neglect some physical effects, however, our analysis indicates that it can well predict the main characteristics of experimental FILD profiles, revealing the underlying mechanism that leads to FI losses.

### Acknowledgments

This work has been carried out within the framework of the EUROfusion Consortium and has received funding from the Euratom research and training programme 2014-2018 and 2019-2020 under grant agreement No 633053. The views and opinions expressed herein do not necessarily reflect those of the European Commission.

### References

- [1] White, R. B. & Chance, M. S. 1984 Phys. Fluids 27, 2455-2467, White, R. B. 2014, The theory of toroidally confined plasmas, 3rd edn. Imperial College Press.
- [2] Antonenas Y, Anastassiou G, Kominis Y, J. Plasma Phys. (2021), vol. 87, 855870101
- [3] M. García-Muñoz et al 2007 Nucl. Fusion 47 L10, M. García-Muñoz et al., Rev. Sci. Instrum. 87, 11D829 (2016), J. Ayllon-Guerola, et al., Fusion Engineering and Design, Volume 123, 2017, Pages 807-810
- [4] J. Galdon-Quiroga et al., PRL 121, 025002 (2018)
- [5] Zestanakis P, Kominis Y, Anastassiou G, Physics of Plasmas 23, 032507 (2016)
- [6] J. Galdon-Quiroga et al 2018 Nucl. Fusion 58 036005